Composites Science and Technology 72 (2012) 1683–1691

Contents lists available at SciVerse ScienceDirect

Composites Science and Technology

journal homepage: www.elsevier.com/locate/compscitech

A multiscale model to describe nanocomposite fracture toughness enhancement by the plastic yielding of nanovoids

Michele Zappalorto, Marco Salviato, Marino Quaresimin *

University of Padova, Department of Management and Engineering, Stradella S. Nicola 3, 36100 Vicenza, Italy

ARTICLE INFO

Article history:
Received 26 March 2012
Received in revised form 9 July 2012
Accepted 10 July 2012
Available online 20 July 2012

Keywords:
A. Nano particles
B. Debonding
B. Interphase
B. Fracture toughness
Plastic yielding

ABSTRACT

The high fracture toughness improvements exhibited by nanofilled polymers is commonly thought of as due to the large amount of energy dissipated at the nanoscale.

In the present work, a multiscale modelling strategy to assess the nanocomposite toughening due to plastic yielding of nanovoids is presented. The model accounts for the emergence of an interphase with mechanical properties different from those of the matrix.

1. Introduction

The recent advances in nanotechnology go towards the production of multi-functional materials through the designing of structures at the nanometer scale. One of the most interesting features concerned with nanocomposites is that they offer exceptional improvements at very low filler concentrations, thus assisting in the achievement of high-level performances across various engineering applications. It is acknowledged that the high fracture toughness improvements exhibited by nanofilled polymers are strictly related to the large amount of energy dissipated by the different damaging mechanisms taking place at the nanoscale. This is the reason for the increasing attention paid in the recent literature to identify nanocomposite damaging mechanisms and to quantify, through models, the related energy dissipation [1–12]. An initial study on the energy dissipation due to the interfacial debonding of nanoparticles has been done by Chen et al. [2]. By means of an energy analysis of the process, these authors derived a simple size-dependent formulation for the debonding stress which was later used to compute the energy dissipation due to this mechanism. The size distribution of particles was thought of as obeying a logarithmic normal distribution and the Weibull distribution function was used to describe the probability of debonding at the interface. The analysis carried out by Chen et al. [2] has been later extended by Zappalorto et al. [3] who developed a closed form expression for the critical debonding stress accounting for the existence of an interphase zone embedding the nanoparticle. Such a zone is thought of as characterised by chemical and physical properties different from those of the matrix, due to inter and supra-molecular interactions taking place at the nanoscale. On parallel tracks, the effects of surface elastic constants on the debonding stress of nanoparticles have been investigated by Salviato et al. [4] who showed that the range of the nanoparticle radii where those effects are significant is limited to the nanoscale. Lauke [5] analysed the energy dissipation phenomena by considering, besides particle debonding, voiding and subsequent yielding of the polymer. Williams [6] re-analysed in detail the toughening of particle filled polymers assuming that plastic void growth around debonded or cavitated particles is the dominant mechanism for energy dissipation. Williams [6] further noted that, even if the debonding process is generally considered to absorb little energy, it is essential to reduce the constraint at the crack tip and, in turn, to allow the epoxy polymer to deform plastically via a void-growth mechanism. A similar result was found also by the present authors in some preliminary analyses [7,8]. Hsieh et al. [9,10] studied the fracture toughness improvements resulting from nanomodification of epoxy resins with silica nanoparticles. Based on experimental observations, they identified two dominant mechanisms responsible of toughening improvements, namely localised shear banding of the polymer (thought of as initiated by the stress concentrations around the periphery of the nanoparticles) and particle debonding followed by subsequent plastic void growth. Conversely, other mechanisms such as crack pinning, crack deflection and immobilised polymer around the particles were not observed. Then, with the aim to predict the fracture toughness improvements resulting

* Corresponding author. Tel.: +39 0444 998723; fax: +39 0444 998888.
E-mail address: marino.quaresimin@unipd.it (M. Quaresimin).

0266-3538/$ - see front matter © 2012 Elsevier Ltd. All rights reserved.
http://dx.doi.org/10.1016/j.compscitech.2012.07.010

from nanomodification, they adapted a previous model due to Huang and Kinloch [13] for rubber modified epoxy polymers. Such a solution, which was proved to be in a very good agreement with the experimental data, requires some quantities to be set on the basis of fracture surface observations. Starting from these experimental observations, it is possible to state that there might be different damaging mechanisms taking place simultaneously at the nanoscale contributing to the overall fracture toughness of the nanocomposite, so that the nanocomposite fracture toughness can be written as $G_{Ic} = G_{Im} + \sum_i \Delta G_i$, where G_{Im} is the fracture toughness of the unloaded matrix and ΔG_i is the fracture toughness improvement due to the ith damaging mechanism. Then, as pointed out recently by these authors [14], the most effective approach to predict the nanocomposite toughness should be a "multi-mechanism" modelling strategy, in which each ΔG_i contribution is appropriately determined and weighted according to the specific case (accounting for the type, the morphology and the functionalisation of the nanofiller as well as of the loading conditions).

Some preliminary analyses in this direction have already been reported in Refs. [7,8]. Those analyses are completed and extended in the present paper, where the multiscale modelling of the toughness improvement due to plastic yielding around nanovoids is addressed.

As a basic hypothesis, it is assumed that debonding of nanoparticles takes place and creates a number of nanovoids of the same diameter of the nanoparticles, which subsequently encounter plastic deformation. This hypothesis is supported by the experimental observations by Hsieh et al. [9,10]. The major novelty of the present paper, with respect to those above mentioned dealing with the same subject [5,6,9,10], lays on the fact that the effect of an interphase zone surrounding the nanoparticle, characterised by mechanical properties different from those of the constituents, is explicitly considered. As shown by Zappalorto et al. [3], the interphase properties, which may be linked to surface functionalizers, have a significant effect on the debonding stress, especially for nanoparticle radii below 50 nm. Briefly, the aims of the present paper can be summarised as follows:

- to prove that nanoparticle debonding can be regarded to absorb little energy, being instead essential to allow the local plastic yielding of the epoxy polymer;
- to quantify the toughness improvement due to the plastic yielding of nanovoids, thought of as nucleated by debonded nanoparticles;
- to show that plastic yielding of nanovoids is a highly dissipative mechanism, causing a high fracture toughness improvement at low nanofiller content;
- to prove that nanocomposite toughening may be strongly affected by the size of nanoparticles and by surface treatments. In particular, the effect of functionalisation is implicitly considered through the properties and the size of the interphase.

The analysis will be carried out considering two different elastic–plastic laws to describe the material behaviour, namely an elastic power hardening law and an elastic perfectly-plastic law. The latter is thought of as a simplified assumption to be used in the absence of detailed information about the hardening behaviour of the matrix and the interphase. It is worth mentioning here again that the correct estimation of the fracture toughness improvement resulting from nanomodification requires the modelling of all the possible damage mechanisms taking place at the nanoscale. Accordingly, this work has to be seen as a first part of a more general multiscale model including the contributions of other mechanisms.

As a further step of the activity in this direction, the present authors are also going to develop a multiscale modelling of the polymer shear banding [15].

2. Description of the hierarchical multiscale strategy adopted for the analysis

2.1. General concepts

A successful engineering application of nanocomposites requires models capable of accounting for their inherent hierarchical structure which encompasses the nano and the macrolength-scales. An effective modelling should take into account the characteristic phenomena of each length-scale and bridge their effects from the smaller scale to the macroscale [14]. For this reason, in the present analysis, we deal with three different length scales, macro-, micro-and nano-, each of them being characterised by mechanical quantities which are, by a conceptual point of view, different. Accordingly, we will use terms like "macroscale stress" and "microscale stress". Thus, in order to avoid misunderstandings it is worth giving the correct definitions for the quantities used at each scale, as well as to briefly discuss the link between them.

The macro-scale system and the macro-scale quantities: the macroscale system is thought of as an amount of material over which all the mechanical quantities (such as stresses and strains) are regarded as averaged values [16] and they are supposed to be representative of the overall material behaviour. Within this scale, it is assumed that the material is homogeneously and continuously distributed over its volume "*so that the smallest element cut from the body possesses the same specific physical properties as the body*" [17]. So long as the geometrical dimensions defining the form of the body are very large in comparison with the dimensions relevant at the smaller scales (such as the size of a single nanofiller), the assumption of homogeneity can be used with great accuracy. In addition, if the nanofiller is randomly oriented and uniformly distributed, the material can also be treated as isotropic.

The macroscale system accounts for the loading conditions and the presence of material defects (like macroscopic cracks) and all the governing equations are dependent only on macroscopic averaged quantities.

The micro-scale system and the micro-scale quantities: the microscale system is thought of as being sufficiently small to be regarded, mathematically, as an infinitesimal volume of the macroscale one. At the same time it has to be, by definition, large enough to be statistically representative of the properties of the material system. The latter hypothesis is supposed to hold valid as far as the nanofiller is uniformly distributed and dispersed over the volume. Within this scale, all the mechanical properties are supposed to be pointwise values [16]. The micro-scale system is often regarded as a *Representative Volume Element* (RVE).

The nano-scale system: the nanoscale system represents a single unit cell of those compounding the micro-scale system; it accounts for the material morphology (such as nanofiller type and size).

It is finally worth mentioning that the definitions above given are not necessarily limited to the analysis of nanostructured materials, but they have a more general validity and they can be applied to any system and application interested by three length scales (a large-scale, a medium-scale and a small-scale) fulfilling the requirement that the "large-scale" is much larger than the "medium-scale", which, in turn, is much larger than "small-scale".

2.2. Relationship between stresses and strains in the different systems

Let consider a general boundary value problem in statics; the macro-scale stress or strain, σ or ε, can be regarded as a general function of material coordinates $\{\sigma, \varepsilon\} = \{f_1(X_1, X_2, X_3), f_2(X_1, X_2, X_3)\}$.

According to [16,18,19], functions f_i, which are supposed to satisfy the governing equations of statics at the macroscale, can

be regarded as an average value over a RVE $\{\sigma,\varepsilon\}=\{\bar{\sigma},\bar{\varepsilon}\}=\left\{\frac{1}{V}\int_V\hat{\sigma}dV,\frac{1}{V}\int_V\hat{\varepsilon}dV\right\}$ where $\hat{\sigma}$ and $\hat{\varepsilon}$ are the micro-scale stress and strain distributions and V is the volume of the RVE. In principle, there might exist an infinite number of $\{\hat{\sigma},\ \hat{\varepsilon}\}$ distributions over the V volume resulting in the same average value, but only one corresponds to the particular boundary value one addresses to. The solution comes from the governing equation and the boundary conditions for this scale which, according to conventional micromechanics, can be expressed, without any loss of generality, within the frame of continuum mechanics.

However, within a multiscale approach to the problem, the knowledge of the correct microscale distributions within the RVE, $\{\hat{\sigma},\ \hat{\varepsilon}\}$, is not strictly necessary. Indeed, the Mori–Tanaka theorem allows to disregard of the actual microscale fields and to approximate the stress or the strain acting on the boundary of a single nano-inhomogeneity (nanoscale). This can be carried out taking advantage of the Global Concentration Tensors of Eshelby diluite solution and of the mean value for the stress/strain fields over the RVE which, in turn, equates the macroscale one.

2.3. Multiscale strategy to analyse debonding of nanoparticles and subsequent plastic yielding

2.3.1. Description of the nanoscale system

In this work particular attention is paid to the interphase zone surrounding the nanoparticle, which might be characterised by chemical and physical properties different from those of the constituents. Indeed, different from traditional microsized composites, in nanoscale materials and structures, the surface effects become significant [20–22], due to the high surface/volume ratio and, for this reason, the amount of interphase volume may represent a large part of the matrix. Recently, Zappalorto et al. [3] developed a closed form expression for the critical debonding stress accounting for the existence of an interphase zone of properties different from those of the matrix. Since different functionalizers lead to different elastic properties of the interphase, this solution shows that the debonding stress is affected by the surface treatment depending also on the interphase radius to the nanoparticle radius ratio, $\mathbf{a}/\boldsymbol{r_0}$.

Unfortunately, the data available so far in the literature about the interphase zone are not enough to precisely formulate the law of variation of its properties across the thickness, as well as its size [23]. Thus, according to [3,24,25], in this work we assume that a through-the-thickness average is representative of the overall property distribution within the interphase. Consequently, the interphase is supposed to be homogeneous and isotropic.

In the light of this, the system under investigation at the nanoscale, shown in Fig. 1a and b, is constituted by:

- a spherical nanoparticle of radius $\boldsymbol{r_0}$, which creates a nanovoid of the same diameter;
- a shell-shaped interphase of external radius $\mathbf{a}$ and uniform properties;
- a matrix of radius $\boldsymbol{b}$ loaded by a hydrostatic stress σ_h, $\boldsymbol{b}$ being much greater than $\boldsymbol{a}$ and $\boldsymbol{r_0}$.

The properties required by the analysis can be computed by means of numerical simulations carried out within the frame of MD as done for example by Odergard et al. [24] and Yu et al. [25], which provide, as outputs, the radial extension of the interphase as well as the elastic properties averaged through the thickness. Alternatively, for a specific system, they could be fitted *a posteriori* on the basis of some experimental results.

2.3.2. Application of the multiscale strategy

Let consider a macrosized crack in a nano-modified matrix (see Fig. 2). In agreement with [6,26,27], it can be assumed that only the hydrostatic stress component of the crack tip stress field is of major importance for the present analysis. This choice is justified by the spherical symmetry of the problem at the nanoscale and the high constraint effects arising close to the crack tip. Indeed, Rice and Tracy [26] showed that, when the mean normal stress is large enough, the volume changing contribution to void growth is much larger than the shape changing part, so that growth is basically spherical.

Under the hypothesis of plane strain conditions, such a component turns to be:

$$\sigma_h=\frac{\sigma_x+\sigma_y+\sigma_z}{3}=\frac{2(1+\nu_o)K_I}{3\sqrt{2\pi\rho}}\cos\frac{\phi}{2} \tag{1}$$

where K_I and ν_o are the Stress Intensity Factor of the macroscopic stress fields and the Poisson's ratio of the nanocomposite, respectively.

Within a multiscale approach to the problem, according to the concepts discussed in Sections 2.1 and 2.2, the macroscale stress, σ_h, can be regarded as the average of the microscale stresses over a RVE (see again Fig. 2). The bridge with the nanoscale can be established by means of the Mori–Tanaka approach, so that the hydrostatic stress component around the nanoparticle can be approximated by:

$$\sigma_n(\rho,\phi)=\frac{\sigma_h}{C_h}=\frac{1}{C_h}\frac{2(1+\nu_o)K_I}{3\sqrt{2\pi\rho}}\cos\frac{\phi}{2} \tag{2}$$

where C_h is the reciprocal of the hydrostatic part of the global stress concentration tensor [3]:

$$C_h=\frac{K_m}{K_p}\zeta \tag{3}$$

with

$$\begin{aligned}\zeta=&\frac{(3K_a+4G_m)(3K_p+4G_a)}{(3K_a+4G_a)(3K_m+4G_m)}+12\\&\times\frac{(K_a-K_p)(G_m-G_a)}{(3K_a+4G_a)(3K_m+4G_m)}\left(\frac{r_0}{a}\right)^3+4\frac{G_m}{K_m}\frac{3K_m+4G_a}{3K_m+4G_m}\\&\times\frac{K_p-K_a}{3K_a+4G_a}\left(\frac{r_0}{b}\right)^3+4\frac{G_m}{K_m}\frac{3K_p+4G_a}{3K_m+4G_m}\frac{K_a-K_m}{3K_m+4G_m}\left(\frac{a}{b}\right)^3\end{aligned} \tag{4}$$

Here K_m, K_a, K_p are the bulk moduli of the matrix, the interphase and the nanoparticle, and G_m, G_a, G_p are the shear elastic moduli of the matrix, the interphase and the nanoparticle. Further accounting for the conditions $b\gg a$, r_0 and $K_p\gg K_m$, K_a, C_h simplifies:

$$C_h=\frac{\xi+4-4\cdot(1-\chi)(r_0/a)^3}{(\xi+4\chi)\left(\frac{3(1-\nu_m)}{1+\nu_m}\right)}=C_{h,0}\frac{\xi+4-4\cdot(1-\chi)(r_0/a)^3}{(\xi+4\chi)} \tag{5}$$

where $\chi=G_a/G_m$, $\xi=3K_a/G_m$ and $C_{h,0}$ is the reciprocal of the hydrostatic part of the global stress concentration tensor evaluated by neglecting the interphase ($\chi=1$).

Debonding at a nanoparticle takes place whenever the hydrostatic stress component around the nanoparticle reaches a critical value, σ_{cr}. Then, the extension of the debonding region (DBR), meant as the region around the crack tip confining all the debonded particles, can be assessed by simply equating σ_n, Eq. (2), with the critical debonding stress σ_{cr}:

$$\sigma_{cr}=\sigma_n(\rho,\phi)=\frac{1}{C_h}\times\frac{2(1+\nu_o)K_I}{3\sqrt{2\pi\rho}}\cos\frac{\phi}{2} \tag{6}$$

In Eq. (6) σ_{cr} can be estimated by [3]:

$$\begin{aligned}\sigma_{cr}&\cong\sqrt{\frac{4\gamma}{r_0}\frac{E_m}{1+\nu_m}}\sqrt{\frac{\chi(4+\xi)-\xi(\chi-1)(r_0/a)^3}{4+\xi+4(\chi-1)(r_0/a)^3}}\\&=\sigma_{cr,0}\sqrt{\frac{\chi(4+\xi)-\xi(\chi-1)(r_0/a)^3}{4+\xi+4(\chi-1)(r_0/a)^3}}\end{aligned} \tag{7}$$

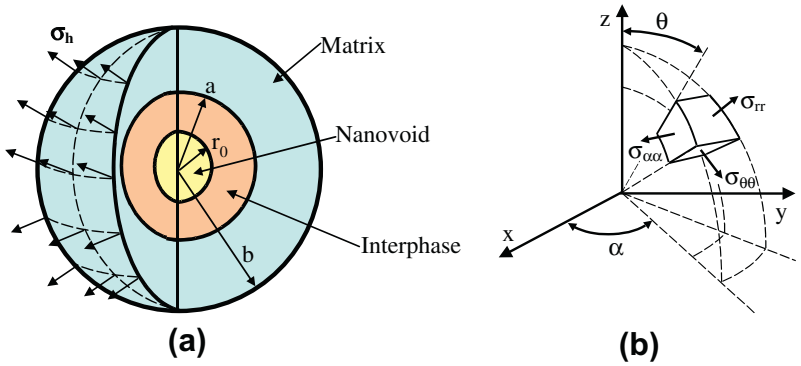

Fig. 1. Description of the system under analysis at the nanoscale (a). Spherical coordinate system and stress components used to describe the stress field around nanovoids (b).

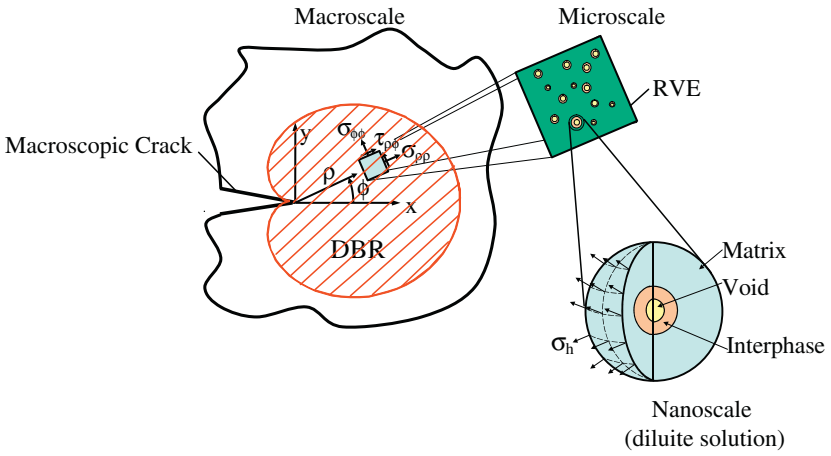

Fig. 2. Description of the multiscale system under analysis.

where $\sigma_{cr,0}$ is the debonding stress evaluated by neglecting the interphase zone [2].

Solving Eq. (6) by ρ results in:

$$\rho^*(\phi) = \frac{1}{(C_h)^2} \times \frac{2(1+v_o)^2 K_I^2}{9\pi\sigma_{cr}^2} \cos^2\left(\frac{\phi}{2}\right) \tag{8}$$

The amount of nanoparticles subjected to debonding, N_p, as well as the total surface subjected to debonding, S_p, can then be calculated as:

$$\begin{aligned} N_p &= \int_V \frac{f_{p0}}{4/3\pi r_0^3} dV = \frac{9}{32}\frac{f_{p0}}{r_0^3}\left[\frac{1}{(C_h)^2}\cdot\frac{2(1+v_0)^2K_1^2}{9\pi\sigma_{cr}^2}\right]^2 \\ S_p &= N_p \times 4\pi r_0^2 = \frac{9}{8}\pi \times f_{p0} \times \frac{A^2}{r_0} \end{aligned} \tag{9a.b}$$

Eq. (9a) can be also re-written in the following normalised form:

$$\frac{N_p}{N_{p,0}} = \left(\frac{C_{h,0}\sigma_{cr,0}}{C_h\sigma_{cr}}\right)^4 \tag{9c}$$

where $N_{p,0}$ is the the amount of nanoparticles subjected to debonding when neglecting the interphase.

In this work, the DBR is thought of as the active process zone. Indeed, it is assumed that the crack-induced stress field causes debonding of nanoparticles, resulting in a distribution of nanovoids which later undergo plastic yielding; both debonding of nanoparticles and the subsequent plastic yielding of nanovoids represent mechanisms acting for energy dissipation at the nanoscale.

It is worth mentioning here that the presence of free volumes in polymers, which might be nanometric in size, can trig nanovoid plastic void growth within the region in between nanoparticles, which is characterised by a high level of dilatational stress. However this phenomenon has not been considered in the present work.

Denoting with U_i the energy produced at the nanoscale for the single mechanism considered, according to the adopted multiscale system, the strain energy density in a RVE (microscale) can be calculated as:

$$u_i = U_i \times \frac{3f_{p0}}{4\pi r_0^3} \tag{10}$$

where f_{p0} is the volume fraction of the nanovoids (which coincides, by hypothesis, with the initial volume fraction of nanoparticles). Finally, the fracture toughness enhancement due to the considered mechanism can be determined, according to [5,13,28,29], as:

$$\Delta G_i = 2 \times \int_0^{\rho^*(\phi=\pi/2)} u_i \, d\rho \tag{11}$$

The problem of determining the overall fracture toughness enhancement is reconverted, in this way into finding the energy produced at the nanoscale by debonding and the plastic yielding of a nanovoid, and thus requires a stress and strain analysis at such scale level.

3. Modelling of debonding-induced toughness improvement

The energy produced at the nanoscale by debonding of a single nanoparticle is:

$$U_{\mathrm{db}} = \gamma_{\mathrm{db}} \times 4\pi r_0^2 \tag{12}$$

where γ_{db} is the interfacial fracture energy. Accordingly, the strain energy density in a RVE (microscale) can be calculated as:

$$u_{db} = U_{db} \times \frac{3f_{p0}}{4\pi r_0^3} = \gamma_{db} \times 4\pi r_0^2 \times \frac{3f_{p0}}{4\pi r_0^3} = 3\frac{\gamma_{db}}{r_0} f_{p0} \tag{13}$$

Finally, the macroscale increment in terms of Strain Energy Release Rate can be estimated by Eq. (11) and turns out to be:

$$\begin{aligned}\Delta G_{db} &= 2 \times \int_0^{\rho^*(\phi=\pi/2)} u_{db} d\rho = 3\frac{\gamma_{db}}{r_0} f_{p0} A \\ &= 3 \times \frac{\gamma_{db}}{r_0} \times \frac{1}{(C_h)^2} \times \frac{2(1+v_o)^2 K_I^2}{9\pi\sigma_{cr}^2} \times f_{p0}\end{aligned} \tag{14}$$

where σ_{cr} is given by Eq. (7).

By further noting that $G = K_I^2/E_o \times (1-v_o^2)$, the toughness improvement due to debonding becomes:

$$\begin{aligned}\Delta G_{db} &= \left\{ \frac{2}{3\pi} \times \frac{\gamma_{db}}{r_0} \times \frac{1+v_o}{1-v_o} \times \frac{E_o}{\sigma_{cr}^2 (C_h)^2} \right\} \times f_{p0} \times G_{Ic} \\ &= f_{p0} \times \psi_{db} \times G_{Ic}\end{aligned} \tag{15}$$

where now G_{Ic} and E_0 are the fracture toughness and the elastic modulus of the nanocomposite and ψ_{db} is the term in curly brackets. Since, according to [5,13], the overall fracture toughness can be written as:

$$G_{Ic} = G_{Im} + \Delta G_{db} \tag{16}$$

being G_{Im} the matrix fracture toughness, Eq. (16) can also be rewritten as:

$$\frac{\Delta G_{db}}{G_{Im}} = \frac{f_{p0} \times \psi_{db}}{1 - f_{p0} \times \psi_{db}} \tag{17}$$

4. Plastic yielding of nanovoids

4.1. Elastic–plastic analysis

Displacement and stress fields are determined here within the frame of the Cauchy Continuum Theory, regarding constituents as isotropic materials, in agreement with some recent works about nanocomposites [2,23,30]. It is assumed that debonding of nanoparticles takes place and creates a number of nanovoids of the same diameter of the nanoparticles. Whenever the stress field around a nanovoid is high enough to cause local yielding, denoting by R_P the extension of the plastic zone, two different conditions are possible:

- the entire interphase and a part of the matrix are yielded ($R_P > a$);
- only a part of the interphase is yielded ($R_P < a$).

To simplify the mathematical treatise to the problem, the first condition is considered. Moreover, in agreement with the "Averaging Stress Concept" [31–33], it is assumed that the "effective macro-scale stress" to be considered in fracture predictions equates the mean value of crack induced stress, σ_h, within the DBR:

$$\sigma_h = \overline{\sigma_h} = \frac{1}{\rho^*(\phi=\pi/2)} \times \int_0^{\rho^*(\phi=\pi/2)} \sigma_h \, d\rho = 2 \times C_h \sigma_{\mathrm{cr}} \tag{18}$$

where the averaging path ($\phi = \pi/2$) matches that suggested in Eq. (11).

4.1.1. A strain hardening behaviour for the interphase and the matrix

When detailed information about the elastic–plastic response of the matrix and the interphase is available, the materials can be thought of as obeying to an elastic-power hardening plastic law.

Thanks to the spherical symmetry of the problem, equilibrium and compatibility equations can be written as:

$$\frac{\partial \sigma_{rr}}{\partial r} + 2 \times \frac{\sigma_{rr} - \sigma_{\theta\theta}}{r} = 0 \tag{19}$$

$$\frac{\partial \varepsilon_{\theta\theta}}{\partial r} = \frac{\varepsilon_{rr} - \varepsilon_{\theta\theta}}{r} \tag{20}$$

The hardening behaviour of materials can be treated in a simplified way by considering an elastic response up to the yield limit σ_Y and thereafter a power law for stresses and strains in the plastic region [34,35]:

$$\begin{cases} \bar{\varepsilon}_P = E \cdot \bar{\sigma}_P & \text{if } \bar{\sigma}_P \leqslant \sigma_Y \\ \frac{\bar{\varepsilon}_P}{\varepsilon_Y} = \left(\frac{\bar{\sigma}_P}{\sigma_Y}\right)^n & \text{if } \bar{\sigma}_P \geqslant \sigma_Y \end{cases} \tag{21}$$

where $\bar{\sigma}_P$ and $\bar{\varepsilon}_P$ are the equivalent stress and the equivalent strain, respectively, while $\varepsilon_Y = \sigma_Y/E$.

Eq. (21) is represented in Fig. 3 for different hardening exponents, n.

Consider the coordinate system shown in Fig. 1b. Hencky's equation links the plastic components of the strains to the plastic components of the stresses [34] and for the law given by Eq. (21) turns out to be:

$$\varepsilon_{ij}^{(pl)} = \lambda s_{ij}^{(pl)} = \frac{3}{2}\frac{\bar{\varepsilon}_P}{\bar{\sigma}_P} s_{ij}^{(pl)} = \frac{3}{2}\frac{\varepsilon_Y}{\sigma_Y}\left(\frac{\bar{\sigma}_P}{\sigma_Y}\right)^{n-1} s_{ij}^{(pl)} \tag{22}$$

where

$$s_{ij}^{(pl)} = \sigma_{ij} - \sigma_h = \sigma_{ij} - \frac{\sigma_{rr} + 2\sigma_{\theta\theta}}{3} \tag{23}$$

is the deviatoric component of stresses. Thanks to the Tresca yielding condition the equivalent plastic stress can be evaluated as:

$$\bar{\sigma}_P = \sigma_{\theta\theta} - \sigma_{rr} \tag{24}$$

Accordingly, the hydrostatic stress component of the plastic stress tensor turns out to be:

$$\sigma_h = \frac{\sigma_{rr} - 2\sigma_{\theta\theta}}{3} = \sigma_{rr}^{(pl)} + \frac{2}{3}\bar{\sigma}_P = \sigma_{\theta\theta}^{(pl)} + \frac{1}{3}\bar{\sigma}_P \tag{25}$$

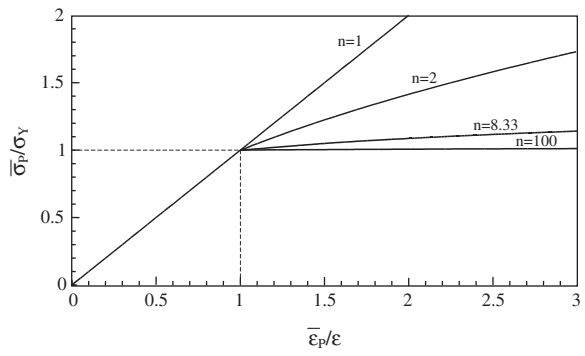

Fig. 3. Simplified stress–strain law for power-hardening material with hardening exponent n.

Then

$$s_{rr}^{(pl)} = \sigma_{rr}^{(pl)} - \sigma_h = -\frac{2}{3}\bar{\sigma}_P \qquad s_{\theta\theta}^{(pl)} = \sigma_{\theta\theta}^{(pl)} - \sigma_h = \frac{1}{3}\bar{\sigma}_P \tag{26a.b}$$

Finally, the plastic strain components are:

$$\varepsilon_{rr}^{(pl)} = \lambda s_{rr}^{(pl)} = -\varepsilon_Y\left(\frac{\bar{\sigma}_P}{\sigma_Y}\right)^n \qquad \varepsilon_{\theta\theta}^{(pl)} = \lambda s_{\theta\theta}^{(pl)} = \frac{1}{2}\varepsilon_Y\left(\frac{\bar{\sigma}_P}{\sigma_Y}\right)^n \tag{27a.b}$$

Substituting Eq. (27) into the compatibility equation, Eq. (20), results in:

$$n\frac{\partial\bar{\sigma}_P}{\partial r} + 3\frac{\bar{\sigma}_P}{r} = 0 \tag{28}$$

The general solution of Eq. (28) can be sought in the form:

$$\bar{\sigma}_P = Cr^{-3/n} \tag{29}$$

At the same time, substituting Eqs. (29) and (24) into the equilibrium equation results in:

$$\sigma_{rr}^{(pl)} = \widetilde{C} - \frac{2}{3}Cn\ r^{-3/n} \tag{30}$$

Then the solutions for stress and displacement fields in the plastic zone are:

$$\sigma_{rr}^{(pl),a} = C_2 - \frac{2}{3}C_1 n_a\ r^{-3/n_a} \qquad \bar{\sigma}_P^a = C_1 r^{-3/n_a} \qquad u^{(pl),a} = \frac{1}{2}\frac{\varepsilon_{Ya}}{r^2}\left(\frac{C_1}{\sigma_{Ya}}\right)^{n_a} \tag{31}$$

when $r < a$ and

$$\sigma_{rr}^{(pl),m} = C_4 - \frac{2}{3}C_3 n_m\ r^{-3/n_m} \qquad \bar{\sigma}_P^m = C_3 r^{-3/n_m} \qquad u^{(pl),m} = \frac{1}{2}\frac{\varepsilon_{Ym}}{r^2}\left(\frac{C_3}{\sigma_{Ym}}\right)^{n_m} \tag{32}$$

when $a < r < R_P$.

Outside the plastic core the behaviour is linear elastic and stress and displacement fields can be described as [3]:

$$\sigma_{rr}^{(el)} = E_m\left[\frac{A}{1-2\nu_m} - 2\frac{B}{r^3(1+\nu_m)}\right] \qquad \sigma_{\theta\theta}^{(el)} = E_m\left[\frac{A}{1-2\nu_m} + \frac{B}{r^3(1+\nu_m)}\right] \qquad u^{(el)} = Ar + \frac{B}{r^2} \tag{33}$$

where E_m and ν_m are the matrix Young modulus and Poisson's ratio.

Boundary conditions to the problem can be written as follows:

$$\begin{aligned}
&\sigma_{rr}^{(pl),a}(r = r_0) = 0\\
&\sigma_{rr}^{(pl),a}(r = a) = \sigma_{rr}^{(pl),m}(r = a)\\
&u^{(pl),a}(r = a) = u^{(pl),m}(r = a)\\
&\bar{\sigma}_P(r = R_P) = \sigma_{Ym}\\
&\sigma_{rr}^{(el),m}(r = b) = \sigma_h\\
&\sigma_{\theta\theta}^{(el),m}(r = R_P) - \sigma_{rr}^{(el),m}(r = R_P) = \sigma_{Ym}\\
&\sigma_{rr}^{(pl),m}(r = R_P) = \sigma_{rr}^{(el),m}(r = R_P)
\end{aligned} \tag{34a.g}$$

The solutions of the first six equations of the previous system are:

$$\begin{aligned}
C_1 &= R_P^{3/n_a}\sigma_{Ya}\left(\frac{\varepsilon_{Ym}}{\varepsilon_{Ya}}\right)^{\frac{1}{n_a}}\\
C_2 &= \frac{2}{3}n_a\sigma_{Ya}\left(\frac{R_p}{r_0}\right)^{3/n_a}\left(\frac{\varepsilon_{Ym}}{\varepsilon_{Ya}}\right)^{\frac{1}{n_a}}\\
C_3 &= R_P^{3/n_m}\sigma_{Ym}\\
C_4 &= \frac{2}{3}\left\{n_a\sigma_{Ya}\left(\frac{R_p}{a}\right)^{3/n_a}\left(\frac{\varepsilon_{Ym}}{\varepsilon_{Ya}}\right)^{\frac{1}{n_a}}\left[\left(\frac{a}{r_0}\right)^{3/n_a} - 1\right] + n_m\sigma_{Ym}\left(\frac{R_p}{a}\right)^{3/n_m}\right\}\\
A &\cong \frac{\sigma_h}{E_m}(1-2\nu_m) = \frac{\sigma_h}{3K_m}\\
B &= \frac{\sigma_{Ym}R_p^3(1+\nu_m)}{3E_m}
\end{aligned} \tag{35a.f}$$

Instead, the last equation can be re-written as:

$$\sigma_h - \frac{2}{3}\sigma_{Ym}(1-n_m) = \frac{2}{3}\left\{n_a\sigma_{Ya}\left(\frac{R_p}{a}\right)^{3/n_a}\left(\frac{\varepsilon_{Ym}}{\varepsilon_{Ya}}\right)^{\frac{1}{n_a}}\left[\left(\frac{a}{r_0}\right)^{3/n_a} - 1\right] + n_m\sigma_{Ym}\left(\frac{R_p}{a}\right)^{3/n_m}\right\} \tag{36}$$

Eq. (36) can be easily solved numerically. Alternatively the assumption $n_m \approx n_a$ results in the following approximation for R_P:

$$R_P = a\cdot\left\{\frac{\frac{3}{2}\frac{\sigma_h}{\sigma_{Ym}} - (1-n_m)}{n_a\frac{\sigma_{Ya}}{\sigma_{Ym}}\left(\frac{\varepsilon_{Ym}}{\varepsilon_{Ya}}\right)^{\frac{1}{n_a}}\left[\left(\frac{a}{r_0}\right)^{3/n_a} - 1\right] + n_m}\right\}^{\frac{n_m}{3}} \tag{37}$$

Substituting Eq. (37) into Eq. (35f) allows one to re-write coefficient B as follows:

$$B = \frac{\sigma_{Ym}R_p^3(1+\nu_m)}{3E_m} = \frac{6\sigma_{Ym}}{G_m}\cdot a^3\cdot\left\{\frac{\frac{3}{2}\frac{\sigma_h}{\sigma_{Ym}} - (1-n_m)}{n_a\frac{\sigma_{Ya}}{\sigma_{Ym}}\left(\frac{\varepsilon_{Ym}}{\varepsilon_{Ya}}\right)^{\frac{1}{n_a}}\left[\left(\frac{a}{r_0}\right)^{3/n_a} - 1\right] + n_m}\right\}^{n_m} \tag{38}$$

In principle, the displacement increase at $r = b$, between the yielded and the un-yielded states, should be equal to:

$$\Delta u \cong \frac{(B-\overline{B})}{b^2} \tag{39}$$

where B is given by Eq. (38) and $\overline{B}$ is, instead [3]:

$$\overline{B} = \sigma_h a^3\frac{4G_a(K_m - K_a) + K_a(4G_a + 3K_m)(r_0/a)^3}{4K_m\left[G_a(4G_m + 3K_a) + 3K_a(G_m - G_a)(r_0/a)^3\right]} \tag{40}$$

However, since $B \gg \overline{B}$, Δu can be reasonably approximated by:

$$\Delta u \cong \frac{B}{b^2} = \frac{6\sigma_{Ym}}{G_m}\cdot\frac{a^3}{b^2}\cdot\left\{\frac{\frac{3}{2}\frac{\sigma_h}{\sigma_{Ym}} - (1-n_m)}{n_a\frac{\sigma_{Ya}}{\sigma_{Ym}}\left(\frac{\varepsilon_{Ym}}{\varepsilon_{Ya}}\right)^{\frac{1}{n_a}}\left[\left(\frac{a}{r_0}\right)^{3/n_a} - 1\right] + n_m}\right\}^{n_m} \tag{41}$$

and the energy produced at the nanoscale by plastic yielding of a single nanovoid results:

$$U_P = F\times\Delta u = 4\pi\sigma_h\frac{6\sigma_{Ym}}{G_m}\cdot a^3\cdot\left\{\frac{\frac{3}{2}\frac{\sigma_h}{\sigma_{Ym}} - (1-n_m)}{n_a\frac{\sigma_{Ya}}{\sigma_{Ym}}\left(\frac{\varepsilon_{Ym}}{\varepsilon_{Ya}}\right)^{\frac{1}{n_a}}\left[\left(\frac{a}{r_0}\right)^{3/n_a} - 1\right] + n_m}\right\}^{n_m} \tag{42}$$

Finally, the strain energy density in a RVE (microscale) can be calculated as:

$$u_P = U_P \times \frac{3f_{p0}}{4\pi r_0^3} = \sigma_h \frac{18\sigma_{Ym}}{G_m} \cdot \left(\frac{a}{r_0}\right)^3 \cdot \left\{ \frac{\frac{3}{2}\frac{\sigma_h}{\sigma_{Ym}} - (1-n_m)}{n_a \frac{\sigma_{Ya}}{\sigma_{Ym}} \left(\frac{\varepsilon_{Ym}}{\varepsilon_{Ya}}\right)^{\frac{1}{n_a}} \left[\left(\frac{a}{r_0}\right)^{3/n_a} - 1\right] + n_m} \right\}^{n_m} f_{p0} \tag{43}$$

4.1.2. Elastic-perfectly plastic behaviour for the interphase and the matrix

In the absence of detailed information about the hardening behaviour of the matrix and the interphase, as a simplified assumption, the materials can be thought of as obeying to an elastic-perfectly plastic law.

To this end, it is easier to reformulate the problem from the beginning, instead than consider this case as the limit condition of the hardening solution for n tending to infinity.

With reference to the coordinate system shown in Fig. 1b, invoking the Tresca yielding criterion, the yielding condition and the equilibrium equation result in [6,36]:

$$\bar{\sigma}_P = \sigma_{\theta\theta} - \sigma_{rr} = \sigma_Y \tag{44}$$

$$\frac{\partial \sigma_{rr}}{\partial r} + 2 \times \frac{\sigma_{rr} - \sigma_{\theta\theta}}{r} = 0 \tag{45}$$

where σ_Y is the material yield stress and $r < R_P$.

Substituting Eq. (44) into Eq. (45) one obtains:

$$\frac{\partial \sigma_{rr}}{\partial r} - 2 \times \frac{\sigma_Y}{r} = 0 \tag{46}$$

The solution for σ_{rr} in the plastic zone is then:

$$\sigma_{rr}^{(pl),a} = C_1 + 2\sigma_{Ya} \cdot Ln(r) \quad \text{when } r < a \tag{47a}$$

$$\sigma_{rr}^{(pl),m} = C_2 + 2\sigma_{Ym} \cdot Ln(r) \quad \text{when } a < r < R_P \tag{47b}$$

where σ_{Ya} and σ_{Ym} are the yield stress of the interphase and of the matrix, respectively. Applying the appropriate boundary conditions, one finally obtains:

$$R_P = a \cdot \left(\frac{r_0}{a}\right)^{\frac{\sigma_{Ya}}{\sigma_{Ym}}} \cdot e^{\left(\frac{\sigma_h}{2\sigma_{Ym}} - \frac{1}{3}\right)} \qquad B = \frac{6\sigma_{Ym}}{G_m} a^3 \cdot \left(\frac{r_0}{a}\right)^{\frac{3\sigma_{Ya}}{\sigma_{Ym}}} \cdot e^{\left(\frac{3\sigma_h}{2\sigma_{Ym}} - 1\right)} \tag{48a.b}$$

So that:

$$\Delta u \cong \frac{(1+\nu_m)\ \sigma_{Ym}}{3E_m} \times \frac{a^3}{b^2} \left(\frac{r_0}{a}\right)^{3 \times \frac{\sigma_{Ya}}{\sigma_{Ym}}} e^{\left(\frac{3\sigma_h}{2\sigma_{Ym}} - 1\right)} \tag{49}$$

The energy produced at the nanoscale by plastic yielding of a single nanovoid is then:

$$U_P = F \times \Delta u = 4\pi\sigma_h \times \frac{(1+\nu_m)\ \sigma_{Ym}}{3E_m} \times a^3 \times \left(\frac{r_0}{a}\right)^{3 \times \frac{\sigma_{Ya}}{\sigma_{Ym}}} e^{\left(\frac{3\sigma_h}{2\sigma_{Ym}} - 1\right)} \tag{50}$$

Accordingly, the strain energy density in a RVE (microscale) can be calculated as:

$$u_P = U_P \times \frac{3f_{p0}}{4\pi r_0^3} = f_{p0} \times \frac{(1+\nu_m)\ \sigma_{Ym}\sigma_h}{E_m} \times \left(\frac{a}{r_0}\right)^{3 \times \left(1 - \frac{\sigma_{Ya}}{\sigma_{Ym}}\right)} \times e^{\left(\frac{3\sigma_h}{2\sigma_{Ym}} - 1\right)} \tag{51}$$

4.2. Fracture toughness enhancement due to plastic yielding of nanovoids

Once the microscale strain energy density has been determined, the macroscale fracture toughness enhancement can be computed by Eq. (11).

The hypothesis formulated at the beginning of Section 4.1 by which $\sigma_h = \bar{\sigma}_h$, with the further substitution $G = K_I^2(1-\nu_o^2)/E_o$, allows one to rewrite Eq. (11) as follows:

$$\Delta G_{py} = 2\rho^*\left(\phi = \frac{\pi}{2}\right) \cdot u_P = \frac{u_P}{(C_h)^2} \cdot \frac{2G_{Ic}}{9\pi\sigma_{cr}^2} \cdot E_o \frac{1+\nu_o}{1-\nu_o} \tag{52}$$

Substituting Eqs. (51) and (43) into Eq. (52) one obtains:

$$\Delta G_{py} = G_{Ic} f_{p0} \left\{ \frac{4}{9\pi C_h} \cdot \frac{E_o}{E_m} \frac{(1+\nu_o)(1+\nu_m)}{1-\nu_o} \frac{\sigma_{Ym}}{\sigma_{cr}} \left(\frac{a}{r_0}\right)^{3 \times \left(1 - \frac{\sigma_{Ya}}{\sigma_{Ym}}\right)} e^{\left(3C_h \frac{\sigma_{cr}}{\sigma_{Ym}} - 1\right)} \right\} = f_{p0} \times \psi_p \times G_{Ic} \tag{53}$$

for the elastic perfectly plastic case, and:

$$\Delta G_{py} = G_{Ic} f_{p0} \left\{ \frac{8}{\pi C_h} \cdot \frac{1+\nu_o}{1-\nu_o} \frac{E_o}{G_m} \frac{\sigma_{Ym}}{\sigma_{cr}} \cdot \left(\frac{a}{r_0}\right)^3 \cdot \left[\frac{3C_h \frac{\sigma_{cr}}{\sigma_{Ym}} - (1-n_m)}{n_a \frac{\sigma_{Ya}}{\sigma_{Ym}} \left(\frac{\varepsilon_{Ym}}{\varepsilon_{Ya}}\right)^{\frac{1}{n_a}} \left[\left(\frac{a}{r_0}\right)^{3/n_a} - 1\right] + n_m} \right]^{n_m} \right\} = f_{p0} \times \psi_p \times G_{Ic} \tag{54}$$

for the power hardening case, respectively. In both cases, ψ_p is the term in curly brackets and quantifies the energy dissipation at the nanoscale by plastic yielding.

Since, according to [28], the overall fracture toughness can be written as:

$$G_{Ic} = G_{Im} + \Delta G_{py} \tag{55}$$

being G_{Im} the fracture toughness of the pure (unloaded) matrix, the fracture toughness improvement due to plastic yielding of nanovoids can be written in the following normalised form:

$$\frac{\Delta G_{py}}{G_{Im}} = \frac{f_{p0} \times \psi_p}{1 - f_{p0} \times \psi_p} \tag{56}$$

5. Results and discussion

In the present work, a general multi-scale approach has been proposed for the damage analysis at the nanoscale induced by the plastic yielding of nanovoids. It has been assumed that the nanofiller is uniformly dispersed and distributed within the volume, agglomeration being neglected at present.

By equating the hydrostatic component of the stress field within the nanoscale to the critical debonding stress, estimated through an expression recently proposed by the authors, Eq. (7), [3] the region containing all the damage due to debonding has been determined in closed form and is given by Eq. (8). This zone, named Debonding Region (DBR), is thought of as the active process zone. Finally, by means of an energy balance, according to [28,29] the fracture toughness improvement related to nanoparticle debonding has been determined.

An example of application of Eq. (17) is reported in Fig. 4, which shows the normalised fracture toughness improvement due to debonding, $\Delta G_{db}/G_{Im}$, versus the nanofiller volume fraction; three different interphase size and properties have been considered. It is evident that, in all cases, the improvement is rather limited (less than 5%). This means that the energy absorbed through nanoparticle debonding is almost negligible.

However, it is quite easy to prove that debonding is a necessary condition for the subsequent plastic yielding around nanovoids created by debonded nanoparticles, such a toughening mechanism being of primary concern. With the aim to prove that, as a first approximation, we can substitute the linear elastic solution for the undebonded particle [3] within the Tresca yielding condition. By so doing, the yielding condition can be written as:

$$\sigma_{rr} - \sigma_{\theta\theta} = \sigma_n \times (1 - 2\nu_a)/(1 - \nu_a) > \sigma_{Ya} \tag{57}$$

where σ_{Ya} is the yield strength of the interphase. As soon as the interphase behaves plastically, ν_a tends to 0.5 and the yielding condition can never be satisfied. This suggests that nanoparticle debonding can be thought of as a "secondary toughening mechanism" being more important as a trigger for plastic yielding [6].

This result is supported by the experimental observation by Hsieh et al. [9,10] and has urged the authors to develop a more insightful analysis, focusing the attention also on the number of nanovoids nucleated from debonding. In Fig. 5 the normalised number of nanovoids predicted by the model, Eq. (9c), is shown as a function of $\mathbf{a/r_0}$. It is evident that the number of possible void grow sites is highly dependent on the interphase properties and that, in particular, softer interphases lead to an higher number of nanovoids.

In the second part of the paper an analysis of the energy spent by the plastic yielding of nanovoids has been carried out. Two different material behaviours have been investigated, the power hardening and the elastic perfectly plastic behaviour. The analysis has highlighted that the elastic and plastic properties of the interphase as well as the nanovoid size play a lead role in the fracture toughness improvements due to this mechanism. In particular the toughness increment to the matrix toughness ratio has been plotted in Fig. 6 as a function of the nanoparticle volume fraction for different values of the nanovoid diameter. The great influence exerted by the nanovoid diameter, d_0, is evident, the ratio $\Delta G_{py}/G_{Im}$ rapidly decreasing as d_0 increases. This strong size effect is in agreement with a large number of experimental results. Differently, Fig. 7 shows the substantial effect of the interphase properties on the fracture toughness improvement. Once again the model agrees with the experimental evidence: as different functionalizers lead to different properties of the interphase, nanocomposite toughening may be strongly affected by surface treatments. It is further important to note that, different from debonding, the plastic yielding of nanovoids is a dominant mechanism for energy dissipation, resulting in high fracture toughness improvements. This is clearly shown in Figs. 6 and 7. An example of the effect of the hardening exponent is finally shown in Fig. 8. The results indicate that the effect of the hardening exponent is, in general, not negligible, higher n values resulting in higher fracture toughness improvements. However, it has to be mentioned that this result strongly depends on the particle and interphase sizes. It is worth mentioning that a correct prediction of the fracture toughness of the nanoparticle filled polymers should include, besides the effect of the plastic yielding of nanovoids, the amount of energy dissipated by the localised shear banding of the polymer (caused by the stress concentrations around the periphery of nanoparticles).

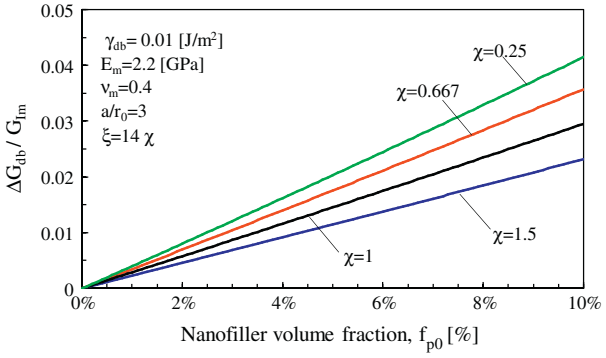

Fig. 4. Plots of $\Delta G_{db}/G_{Im}$ according to Eq. (15) versus the nanofiller volume fraction. The bulk material properties match those of the epoxy resin used by Chen et al. [2].

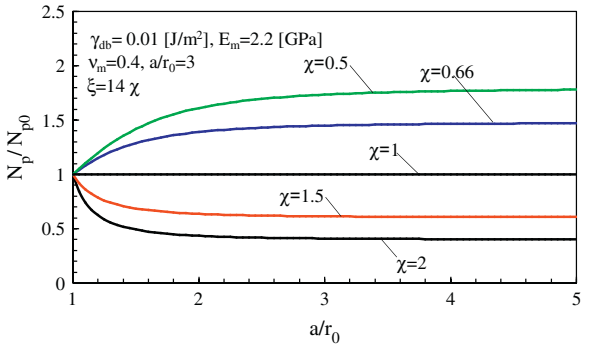

Fig. 5. Influence of the interphase size and properties on the normalised amount of debonded nanoparticles, $N_p/N_{p,0}$. The bulk material properties match those of the epoxy resin used by Chen et al. [2].

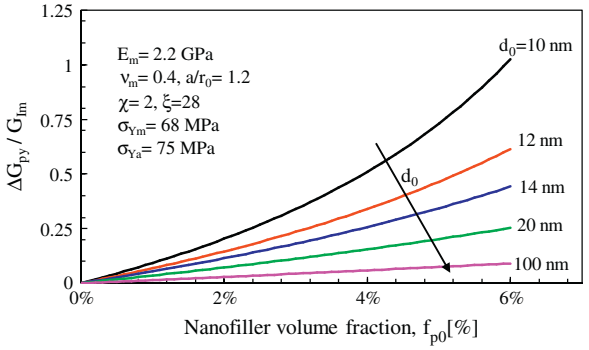

Fig. 6. Plots of $\Delta G_{py}/G_{Im}$ according to Eq. (53) versus the nanofiller volume fraction; nanovoid of different diameter, d_0. The bulk material properties match those of the epoxy resin used by Chen et al. [2].

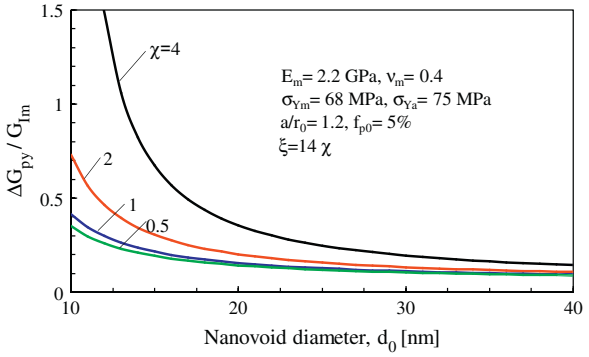

Fig. 7. Plots of $\Delta G_{py}/G_{Im}$ according to Eq. (53) versus the nanovoid diameter: different interphase properties. The bulk material properties match those of the epoxy resin used by Chen et al. [2].

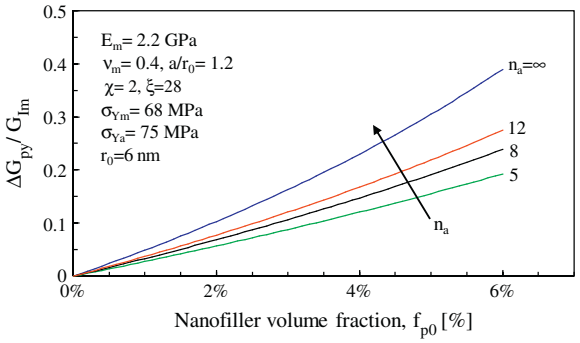

Fig. 8. Influence of the hardening exponent on the $\Delta G_{py}/G_m$ ratio, according to Eqs. (53) and (54).

This last mentioned mechanism is not dealt with in this paper, the mechanics of damage being much different with respect to that of the plastic yielding (see also [9,10]). As a consequence, the assessments based solely on the multiscale model developed in this work will inevitably result in an underestimation of the fracture toughness for nanoparticle filled polymers. This is the reason why a direct comparison with experimental results is not reported here. Moreover one should note that, as a basic assumption of the present work, the nanofiller is supposed to be uniformly dispersed and distributed, neglecting the high tendency to agglomerate exhibited by nanoparticles beyond a certain value of the volume fraction. It is clear that this approximation limits the application of the model to low nanofiller volume fractions.

6. Conclusions

The present work provides a hierarchical multi-scale model to assess the toughness improvement due to plastic yielding around nanovoids, thought of as nucleated by debonding of nanoparticles. Neglecting, for the time being, possible effects of nanofiller agglomeration, the inter- and supra-molecular interactions between nanofillers and the polymer are accounted for by introducing an interphase embedding the nanovoid, with mechanical properties different from those of the matrix. It has been shown that plastic yielding is a highly dissipative mechanism, causing a high fracture toughness improvement at low nanofiller content. Finally it has been shown that nanocomposite toughening may be strongly affected by the size of nanoparticle and surface treatments.

Acknowledgements

The financial support to the activity by Veneto Nanotech, the Italian Cluster of Nanotechnology (Padova, Italy), is greatly acknowledged.

References

[1] Wetzel B, Rosso P, Haupert F, Friedrich K. Epoxy nanocomposites–fracture and toughening mechanisms. Eng Fract Mech 2006;73:2375–98.
[2] Chen JK, Huang ZP, Zhu J. Size effect of particles on the damage dissipation in nanocomposites. Compos Sci Technol 2007;14:2990–6.
[3] Zappalorto M, Salviato M, Quaresimin M. Influence of the interphase zone on the nanoparticle debonding stress. Compos Sci Technol 2011;72:49–55.
[4] Salviato M, Zappalorto M, Quaresimin M. The effect of surface stresses on the critical debonding stress around nanoparticles. Int J Fract 2011;172:97–103.
[5] Lauke B. On the effect of particle size on fracture toughness of polymer composites. Compos Sci Technol 2008;68:3365–72.
[6] Williams JG. Particle toughening of polymers by plastic void growth. Compos Sci Technol 2010;70:885–91.
[7] Salviato M, Zappalorto M, Quaresimin M. Plastic yielding around nanovoids. Procedia Eng 2011;10:3316–21.
[8] Zappalorto M, Salviato M, Quaresimin M. Assessment of debonding-induced toughening in nanocomposites. Procedia Eng 2011;10:2982–7.
[9] Hsieh TH, Kinloch AJ, Masania K, Taylor AC, Sprenger S. The mechanisms and mechanics of the toughening of epoxy polymers modified with silica nanoparticles. Polymer 2010;51:6284–94.
[10] Hsieh TH, Kinloch AJ, Masania K, Sohn Lee J, Taylor AC, Sprenger S. The toughness of epoxy polymers and fibre composites modified with rubber microparticles and silica nanoparticles. J Mater Sci 2010;45:1193–210.
[11] Johnsen BB, Kinloch AJ, Mohammaed RD, Taylor AC, Sprenger S. Toughening mechanisms of nanoparticle-modified epoxy polymers. Polymer 2007;48:530–41.
[12] Zhao S, Schadler LS, Duncan R, Hillborg H, Auletta T. Mechanisms leading to improved mechanical performance in nanoscale alumina filled epoxy. Compos Sci Technol 2008;68:2965–75.
[13] Huang Y, Kinloch AJ. Modelling of the toughening mechanisms in rubber-modified epoxy polymers. Part II: A quantitative description of the microstructure–fracture property relationships. J Mater Sci 1992;27:2763–9.
[14] Quaresimin M, Salviato M, Zappalorto M. Strategies for the assessment of nanocomposite mechanical properties. Compos Part B-Eng 2012;43:2290–7.
[15] Salviato M, Zappalorto M, Quaresimin M. A multiscale analytical model to assess fracture toughness improvements due to plastic shear bands. In: Proceedings of the 15th European conference on composite materials, ECCM 15, Venice, Italy, 24–28, June 2012.
[16] Bishop JFW, Hill R. A theory of the plastic distortion of a polycrystalline aggregate under combined stresses. Philos Mag Ser 7 1951;42:414–27.
[17] Timoshenko SP, Goodier JN. Theory of elasticity. third ed. New York: McGraw-Hill; 1970.
[18] Hutchinson JW. Plastic stress–strain relation of FCC polycrystalline metals hardening according to Taylor's rule. J Mech Phys Solids 1964;12:11–24.
[19] Gurson AL. Continuum theory of ductile rupture by void nucleation and growth: Part I – yield criteria and flow rules for porous ductile media. J Eng Mater Technol 1977;99:2–15.
[20] Ajayan PM, Schadler LS, Braun PV. Nanocomposite science and technology. Wiley-VCH; 2003. ISBN 3527303596.
[21] Wichmann MHG, Cascione M, Fiedler B, Quaresimin M, Schulte K. Influence of surface treatment on mechanical behaviour of fumed silica/epoxy resin nanocomposites. Compos Interfaces 2006;13:699–715.
[22] Tian L, Rajapakse RKND. Elastic field of an isotropic matrix with a nanoscale elliptical inhomogeneity. Int J Solids Struct 2007;44:7988–8005.
[23] Sevostianov I, Kachanov M. Effect of interphase layers on the overall elastic and conductive properties of matrix composites. Applications nanosize inclusion. Int J Solids Struct 2007;44:1304–15.
[24] Odegard GM, Clancy TC, Gates TS. Modeling of mechanical properties of nanoparticle/polymer composites. Polymer 2005;46:553–62.
[25] Yu S, Yang S, Cho M. Multi-scale modeling of cross-linked epoxy nanocomposites. Polymer 2009;50:945–52.
[26] Rice JR, Tracy DM. On ductile enlargement of voids in triaxial stress fields. J Mech Phys Solids 1969;17:210–7.
[27] McMeeking RM, Evans AG. Mechanics of transformation-toughening in Brittle materials. J Am Ceram Soc 1982;65:242–6.
[28] Freund LB, Hutchinson JW. High-strain-rate crack growth in rate dependent plastic solids. J Mech Phys Solids 1985;33:169–91.
[29] Evans AG, Williams S, Beaumont PWR. On the toughness of particulate filled polymers. J Mater Sci 1985;20:3668–74.
[30] Boutaleb S, Zaıri F, Mesbah A, Naït-Abdelaziz M, Gloaguen JM, Boukharouba T. Micromechanics-based modelling of stiffness and yield stress for silica/polymer nanocomposites. Int J Solids Struct 2009;46:1716–26.
[31] Wieghardt K. Über das Spalten und Zerreiβen elastischer Körper. Z Math Phys 1907;55:60–103. translated in English by H.P. Rossmanith, Fatigue Fract Engng Mater Struct 1995; 18: 1371–1405.
[32] Neuber H. Kerbspannungslehre. 2nd ed. Berlin: Springer; 1958.
[33] Neuber H. Über die Berücksichtigung der Spannungskonzentration bei Festigkeitsberechnungen. Konstruktion 1968;20:245–51.
[34] Chakrabarty J. Theory of plasticity. 3rd ed. Oxford, UK: Butterworth-Heinemann Publication; 2006.
[35] Lazzarin P, Zappalorto M. Plastic notch stress intensity factors for pointed V-notches under antiplane shear loading. Int J Fract 2008;152:1–25.
[36] Kachanov LM. Fundamentals of the theory of plasticity. Amsterdam, Netherlands: North Holland publishing company; 1971.